Noise Reduction in Periodically Switching MOSFET Circuits Using Iteratively Found Synthesized Control Signals

Tobias Dörlemann, Andreas Bendicks, Caroline Krause, Stephan Frei
TU Dortmund University, On-board Systems Lab
Dortmund, Germany
tobias.doerlemann@tu-dortmund.de

***Abstract*—In many modern power electronic systems, fast periodically switching semiconductors are utilized for system control and minimizing switching losses. The resulting steep switching waveforms may cause electromagnetic interference (EMI) that is mostly reduced with help of heavy passive filter circuits. One basic idea is to optimize EMC behavior and efficiency of power electronic devices by forming the switching waveforms with regard to steepness, overshoots, ringing and high frequency disturbances. Therefore, optimum control signals have to be found and synthesized. To do so, the nonlinear transmission behavior of semiconductor devices has to be considered. To start with, a basic MOSFET test circuit is regarded in this work. With help of an iterative search algorithm, a control signal is found that fits the MOSFET's output signal to a desired waveform that optimizes EMI and minimizes switching losses. The capability of this method is shown by simulations and measurements.**

Keywords—power electronics, semiconductors, switching losses, gate control, synthesized control signals, nonlinear systems, optimization

I. Introduction

In hybrid electric vehicles (HEV) and electric vehicles (EV), power electronic converters are relevant sources of electromagnetic interference (EMI). Inside these converters, hardly switched transistors cause steep switching waveforms. While switching speed is increased to optimize efficiency, the resulting steep switching waveforms contain high frequency components that may cause EMI problems. Hence, a trade-off between EMC behavior and efficiency has to be made.

Evolving from conventional gate drives with constant resistances and voltage step-functions at the transistor's gate, the concept of active gate driving has been developed to control the steep switching waveforms of power electronic devices [1]-[7]. Hereby, a trade-off between EMI and the converter's efficiency can be achieved. Active gate driving is realized in form of different approaches. In [1] and [2] the gate resistance is varied during the switching process according to a previously programmed scheme. In [3] the gate-source voltage is fed back in order to control the gate resistance. The approach presented in [4] proposes to feed back the drain current's gradient and to impress a gate current with help of a controlled current source. In [5]-[7], an additional current is impressed to the transistor's gate with help of an inductive transducer between the transistor's source path and its gate path. Hereby, the switching speed can be increased, while the switching losses are decreased.

In [8] and [9], the disturbing harmonics of a power electronic converter are suppressed by superposing them with synchronized and synthesized cancellation signals. While doing so, there is no significant effect on the dc/dc converter's efficiency. The cancellation signals are injected with help of passive injecting circuits that can be assumed to be linear time invariant (LTI) systems. As a result, the superposition principle allows a simple harmonic-wise interference of the noise and the anti-noise signal. Moreover, this method does not require an exact knowledge of the dc/dc converter's transmission behavior.

In contrast, the approaches presented in [10] and in this document consider the nonlinear relationship between the gate-source voltage and the drain-source voltage of a simple MOSFET test circuit. Because the identification of a nonlinear system behavior may be quite extensive, an iterative search method is proposed. While varying the test circuit's input signal, its output signal is fitted to a desired waveform that may optimize both, EMI and efficiency.

At first, the theoretical background is explained in chapter II. In chapter III, the utilized iterative optimization algorithm is described. In chapter IV and V, this optimization algorithm is applied to a simulation and a measurement test setup, respectively. Finally, a conclusion and an outlook are given in VI.

II. Theoretical Background

In general, semiconductor devices show a nonlinear system behavior. In contrast to linear time invariant systems (LTI), a nonlinear system's output signal does not exclusively contain those frequency components that its input signal consists of. In case of a memoryless nonlinear system, harmonic frequencies and intermodulation products need to be considered. Fig. 1 (top) depicts a nonlinear system with an input signal $y_1(t)$, an output signal $y_2(t)$ and the system function F.

A simple example for a nonlinear system is a quadratic dependency between an input signal $y_1(t)$ and an output signal $y_2(t)$. If an input signal consists of two angular frequency components ω_0 and $2\omega_0$ it can be written, using complex Fourier series, as shown in (1) with the Fourier coefficients c_{1_n}.

$$y_1(t) = \sum_{n=-2}^{2} c_{1_n} e^{jn\omega_0 t} \tag{1}$$

$2\omega_0$ can be seen as the second harmonic of the fundamental frequency ω_0. A simple square system function gives (2).

$$y_2(t) = \left(y_1(t)\right)^2 = y_1^2(t) = \sum_{n=-2}^{2} c_{1_n} e^{jn\omega_0 t} \cdot \sum_{l=-2}^{2} c_{1_l} e^{jl\omega_0 t} = \sum_{n=-2}^{2} \sum_{l=-2}^{2} c_{1_n} c_{1_l} e^{j(n+l)\omega_0 t} \tag{2}$$

As it can be seen, all multiple frequencies of ω_0 will appear up to $(n+l)\omega_0 = 4\,\omega_0$.

This can be generalized to higher powers k and excitations with a larger number of frequency components, $\omega_0, 2\omega_0, \ldots, N\omega_0$.

$$y_1^k(t) = \sum_{n_1=-\mathrm{N}}^{\mathrm{N}} \sum_{n_2=-\mathrm{N}}^{\mathrm{N}} \ldots \sum_{n_k=-\mathrm{N}}^{\mathrm{N}} \prod_{i=1}^{k} c_{1_{n_i}} e^{j\omega_0 t \sum_{i=1}^{k} n_i} \tag{3}$$

In general, any memoryless nonlinear system can be described by a polynomial of order K with the coefficients a_k.

$$y_2(t) = \sum_{k=0}^{\mathrm{K}} a_k\, y_1^k(t) \tag{4}$$

$$y_2(t) = \sum_{k=0}^{\mathrm{K}} \sum_{n_1=-\mathrm{N}}^{\mathrm{N}} \sum_{n_2=-\mathrm{N}}^{\mathrm{N}} \ldots \sum_{n_k=-\mathrm{N}}^{\mathrm{N}} a_k \prod_{i=1}^{k} c_{1_{n_i}} e^{j\omega_0 t \sum_{i=1}^{k} n_i} \tag{5}$$

It can be seen that only multiples of ω_0 have to be expected. With an input signal consisting of N harmonics and a system function that can be written as polynomial of K-th order, $N \cdot K$ frequency components can be expected. The highest output frequency is $\omega_{2_{\max}}$.

$$\omega_{2_{\max}} = N \cdot K \cdot \omega_0 \tag{6}$$

This means, depending on the degree of nonlinearity with a wide band input signal, a very wide band output signal might appear. It can be also seen, that the highest frequencies are weighted with the highest $c_{1_{n_i}}$. If an input signal is low pass filtered, i.e. the Fourier coefficients $c_{1_{n_i}}$ drop with higher frequencies, also the output signal, i.e. the intermodulation frequencies will drop at higher frequencies.

As it can be seen in Fig. 1 (bottom), the output signal $y_2(t)$ of this nonlinear system consists of harmonic and intermodulation frequencies up to $N \cdot K \cdot \omega_0 = 4\omega_0$.

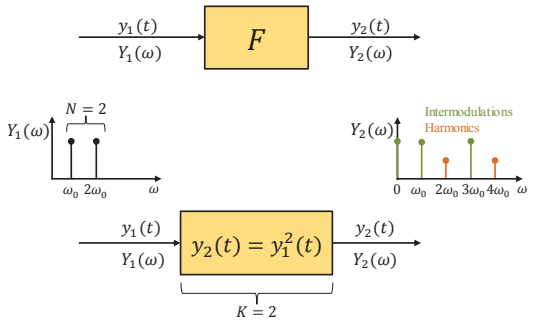

Fig. 1. A quadratic (K=2) nonlinear system F with input signal $y_1(t)$ with two frequency components (N=2) and output signal $y_2(t)$ (top). Stimulation leads to harmonics and intermodulation in the output signal (bottom).

Because of the intermodulation effect and the occurring harmonics in the nonlinear system's output signal, the optimization of the input signal regarding undesired output signal frequencies is no trivial task. In the following, a simple optimization strategy is described.

III. Optimization Strategy

The main advantage of an iterative search for an optimal control signal is that no system identification is needed. Hereby, no thermal or frequency-dependent behavior, e.g. by frequency-dependent parasitic capacitances, needs to be known in advance.

As it is already depicted in Fig. 1 (top), the nonlinear system behavior is represented by the system function F that links the input signal $y_1(t)$ with the output signal $y_2(t)$. The regarded optimization strategy bases on a variation of the input signal $y_1(t)$ while the resulting output signal $y_2(t)$ is compared to a desired output signal $y_{2,\mathrm{target}}(t)$. By iteratively modifying $y_1(t)$, the resulting output signal $y_2(t)$ is fitted to $y_{2,\mathrm{target}}(t)$.

Both signals $y_1(t)$ and $y_2(t)$ are assumed to be periodic. In addition, the system's output signal is assumed to solely contain angular frequency components that are integer multiples of the input signal's fundamental angular frequency ω_0. Therefore, the system's input signal $y_1(t)$ and its output signal $y_2(t)$ can be represented as Fourier series.

A. Determination of a demanded output signal

The proposed optimization algorithm is based on the specification of a desired output signal $y_{2,\mathrm{target}}(t)$ and the choice of an appropriate cost function J. Generally, the formulation of a demanded output signal, as well as the evaluation with help of a cost function can be done in time or in frequency domain. In the following, the cost function is chosen to evaluate time domain signals, as shown in (7).

$$J = \mathrm{rms}\left(y_{2,\mathrm{target}}(t) - y_2(t)\right) \tag{7}$$

First, it is assumed that the nonlinear system is controlled by a hard-switched control signal, e.g. a trapezoidal pulse. Based on the resulting output signal, a desired output signal $y_{2,\mathrm{target}}(t)$ is formulated. To do so, the spectrum of the resulting output signal is calculated with help of the Fast Fourier Transform (FFT). Now, the desired output signal is formulated in frequency domain, such that it meets the desired requirements.

After an Inverse Fast Fourier Transform (IFFT) of the desired output signal $Y_{2,\mathrm{target}}(\omega)$, the time domain signal $y_{2,\mathrm{target}}(t)$ is available. While doing so, it is important to ensure the target output signal $y_{2,\mathrm{target}}(t)$ to be physical. The concept of determining a desired output signal is depicted in Fig. 2.

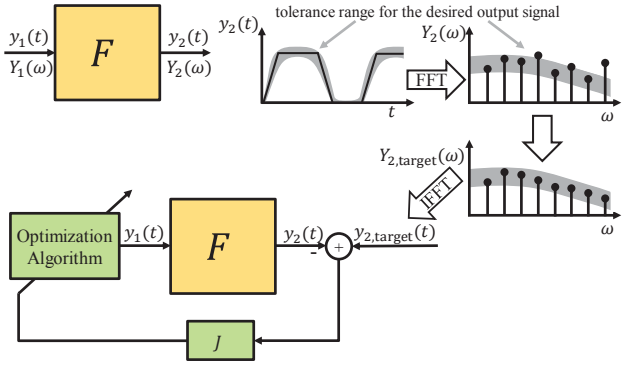

Fig. 2. Determination of a target output signal.

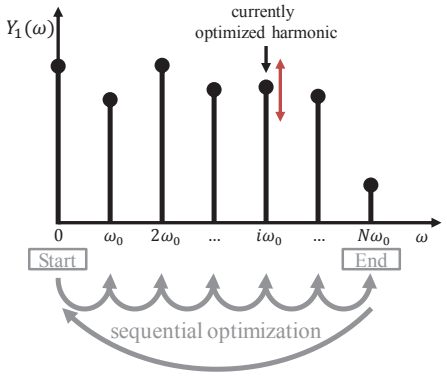

Fig. 3. Sequential optimization of the control signal.

B. *Description of the optimization task*

The finding of the needed control signals is described now. In case of an unknown nonlinear system, a mutual influence of all input harmonics towards the output signal has to be taken into account. As the number of harmonics can be infinite, it is further assumed that there is an upper frequency limit. Above this limit the harmonics can be neglected or a simple analog filter becomes effective. The more frequency components are allowed in $y_1(t)$, the larger the parameter range becomes, and the longer a search optimization takes. In the following, it is assumed that $y_1(t)$ at most includes all frequency components that $y_{2,\text{target}}(t)$ consists of, which is an experience-based assumption. The input signal $y_1(t)$ is represented as a Fourier series with fundamental angular frequency $\omega_0 = 2\pi f_0$, which equals the fundamental angular frequency of the desired output signal.

$$y_1(t) = \sum_{i=0}^{N} [A_\text{i} \cdot \cos(i\omega_0 t) + B_\text{i} \cdot \sin(i\omega_0 t)] \qquad (8)$$

Obviously, two parameters per frequency component of $y_1(t)$ have to be optimized, while only one parameter is needed to parametrize the DC offset. Overall, $2N + 1$ parameters need to be optimized. The fact that a mutual affection of the input signal's harmonics on the output signal needs to be taken into account, increases the complexity of the optimization problem significantly. A detailed estimation of the required optimization effort is shown in E.

C. *Sequential Optimization Approach*

During the optimization, all $2N + 1$ parameters A_i and B_i of $y_1(t)$ are adapted such that the output signal $y_2(t)$ ideally equals the demanded output signal $y_{2,\text{target}}(t)$. Therefore, all frequency components $0 \leq i\omega_0 \leq N\omega_0$ of $y_1(t)$ need to be optimized regarding their A_i and B_i. Because the system function F is assumed to be nonlinear, the superposition principle is not valid. As a result, the frequency components of $y_1(t)$ cannot be optimized separately. To find a solution for the problem, a sequential optimization of the frequency components of $y_1(t)$ is chosen, starting with the DC value of $y_1(t)$. After the harmonic $N \cdot \omega_0$ of $y_1(t)$ is optimized, the proposed algorithm starts with the DC value of $y_1(t)$ again. In this manner, the optimization algorithm sequentially sweeps through the allowed input signal frequency components several times. The input harmonics are superposed and generate a combined output signal.

D. *Determination of the control signal*

In case of an unknown nonlinear system, the input signal's frequency components can mutually affect each other on the output signal. Therefore, every frequency component of $y_1(t)$ is ideally optimized several times. Hence, the amount of iterations per optimized frequency component should be minimized. To do so, a parameter grid as shown in Fig. 4 is created for the currently regarded i-th harmonic of $y_1(t)$. For every parameter combination (A_i, B_i) that is represented by an orange dot in Fig. 4, the i-th harmonic of the input-sided control signal is created and superposed with all previously optimized input frequency components. For every parameter combination, the cost function J is evaluated. For illustration purposes, the parameter combination that leads to the minimum cost function value, while optimizing the i-th harmonic of $y_1(t)$, is exemplarily marked by the blue cross in Fig. 4 and Fig. 5, respectively. The red cross represents the optimal parameter combination.

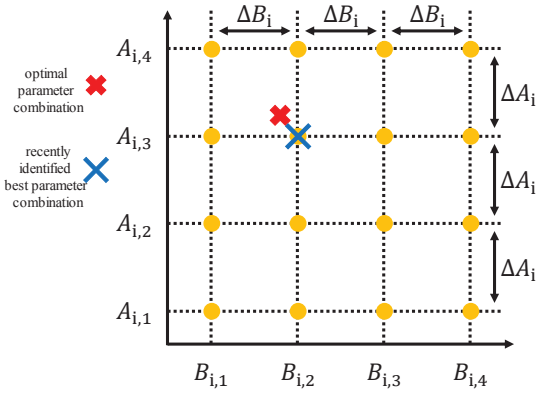

Fig. 4. Parameter net for optimization of the i-th input frequency component.

In the next step, a new parameter net is located around the recently identified optimal parameter set. The resulting parameter combinations are visualized by the red dots in Fig. 5. While comparing Fig. 4 and Fig. 5, it can easily be seen that the parameter resolution of ΔA_i and ΔB_i, respectively, is improved with every refinement of the parameter net. In that iterative manner, the optimal parameter combination of the i-th frequency component is found with increasing precision. Therefore, a specific number of parameter net refinements is required. The more refinements are made, the higher is the suppression.

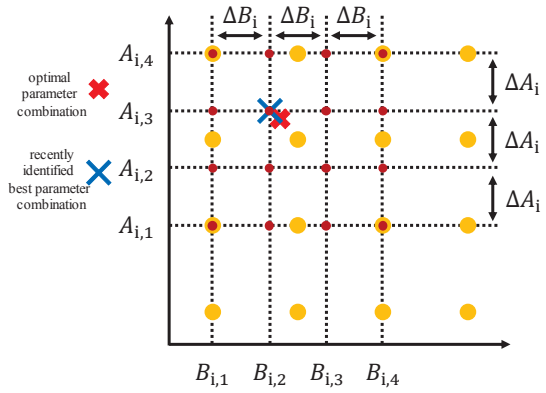

Fig. 5. Refined parameter net for optimization of the i-th frequency component.

E. Estimation of the optimization effort

During optimization, $2N + 1$ parameters are optimized in X sweeps. For each of the $N + 1$ frequency components, 16 parameter combinations that are represented by the dots in Fig. 4 and Fig. 5 need to be tested. Here, the number of parameter net refinements R needs to be considered. As a result, the overall number of parameter combinations Z that are needed to test for optimizing the nonlinear system's input signal $y_1(t)$ outcomes to (9).

$$Z = X \cdot (N + 1) \cdot (R + 1) \cdot 16 \tag{9}$$

IV. Simulation

In the following, the previously described optimization strategy is applied to a simulation model which contains a switching NMOS source circuit depicted in Fig. 6. The used NMOS model represents a simple n-channel MOSFET's current-voltage characteristic and comprises subthreshold, ohmic and saturation mode. This basic circuit set-up provides a basis for future investigations towards applications on dc/dc converters.

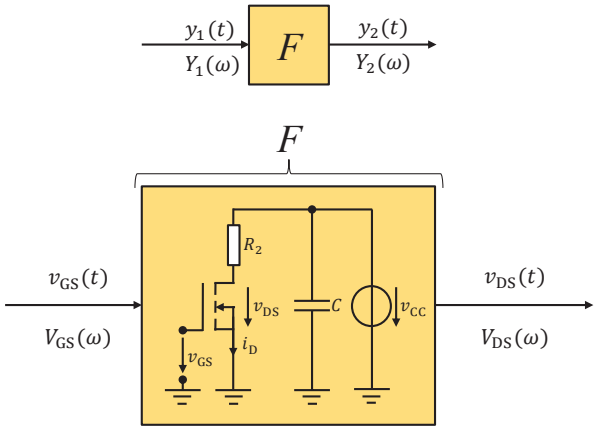

Fig. 6. NMOS source circuit with the NMOS representing the nonlinear system. The gate-source voltage and drain-source voltage represent its input and output signal.

A. Determination of the demanded output signal

In a first step, the desired output signal $v_{DS,target}(t)$ has to be defined. To do so, the MOSFET model is controlled first by a trapezoidal input signal $v_{GS}(t)$ with period $T = 1/f_0$. The fundamental angular frequency is chosen to $\omega_0 = 2\pi f_0$ with $f_0 = 100\,\text{kHz}$. The upper graph in Fig. 7 shows the trapezoidal control signal $v_{GS}(t)$ with a period $T = 1/f_0 = 10\,\mu\text{s}$ and the resulting drain-source voltage $v_{DS}(t)$. The lower graph in Fig. 7 represents the calculated spectrum $V_{DS}(f)$ of the MOSFET's drain-source voltage with $f = \omega / 2\pi$. Based on this output spectrum, a desired output signal $v_{DS,target}(t)$ can be defined. In this example, $v_{DS,target}(t)$ should consist of only the first 10 harmonics of $v_{DS}(t)$. All other frequency components should be zero. The Gibbs phenomenon states that the missing frequency components of the original output spectrum lead to an over- and/or undershooting of the demanded time domain signal $v_{DS,target}(t)$, compared with the original time domain signal $v_{DS}(t)$. As it can be seen in Fig. 6, $v_{DS}(t)$ is limited by the source circuit's supply voltage v_{CC}. Therefore, to ensure the desired output signal's physicality, a small reduction of its DC-Offset needs to be enforced. The undershoots of the desired output signal $v_{DS,target}(t)$ do not lead to an unphysical demand, as long as the resulting drain current is smaller than its maximum possible value which is limited by v_{CC}, R_2 and the MOSFET's $R_{DS(on)}$. During the optimization, the given frequency components of $v_{GS}(t)$, which range from DC to $10f_0$ $(N = 10)$, are optimized ten times $(X = 10)$ sequentially. During the optimization of the i-th frequency component of $v_{GS}(t)$, the parameter net is refined thirty times $(R = 30)$. With (9), the resulting quantity of tested parameter combinations results in $Z = 54560$. Hereby, the minimum value of the cost function J can be found quite precisely.

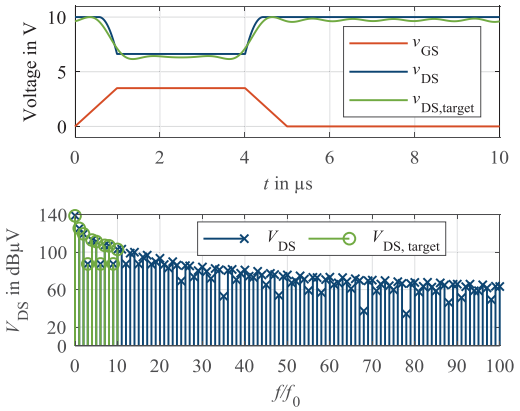

Fig. 7. Simulation: trapezoidal $v_{GS}(t)$, resulting $v_{DS}(t)$ and demanded $v_{DS,target}(t)$ (top). Comparison of the resulting spectra of the original $V_{DS}(f)$ (bottom, blue) and the demanded output signal $V_{DS,target}(f)$ (bottom, green).

B. Simulation results

Regarding the upper graph in Fig. 8, the optimized drain-source voltage is highly related to the desired drain-source voltage. Considering the spectrum of both signals, the optimized $V_{DS,optimized}(f)$ consists of discrete frequency components in range from DC to $20f_0$. Compared to the desired drain-source voltage spectrum $V_{DS,target}(f)$ in Fig. 7, which is composed by frequency components in range from DC to $10f_0$, there is a significant difference which is caused by the nonlinear behavior of the MOSFET model. The MOSFET model can be assumed to be predominantly quadratic $(K = 2)$. The input signal is assumed to consist of frequency compo-

nents from DC to $10f_0$ ($N = 10$). With help of (6), the maximum frequency component of the nonlinear systems output signal can be calculated and results to $20f_0$. Therefore, the resulting frequency components $11f_0$ to $20f_0$ of $v_{\mathrm{DS,optimized}}(t)$ are plausible.

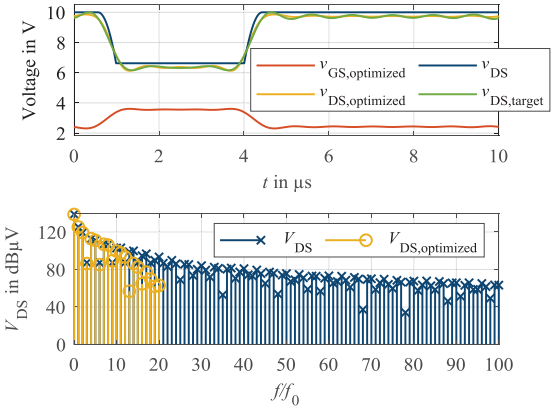

Fig. 8. Simulation: optimized $v_{\mathrm{GS,optimized}}(t)$, resulting $v_{\mathrm{DS,optimized}}(t)$ compared to the original $v_{\mathrm{DS}}(t)$ and the demanded $v_{\mathrm{DS,target}}(t)$ in time domain (top). Spectra of the original $V_{\mathrm{DS}}(f)$ and the optimized $V_{\mathrm{DS,optimized}}(f)$ (bottom).

In conclusion, the proposed iterative algorithm is able to find a suitable gate-source voltage to fit the NMOS model's drain-source voltage to a given time domain signal. In the following, the proposed iterative search algorithm is applied to a real system.

V. Measurement

To demonstrate the capability of the proposed optimization algorithm, a simple MOSFET source circuit is utilized. This demonstrator is embedded into a measurement environment consisting of an oscilloscope that measures the drain-source voltage, an arbitrary function generator with an internal resistance $R_{\mathrm{i}} = 50\ \Omega$ and a PC running the optimization algorithm. Fig. 9 depicts the measurement test setup, which is summarized in Fig. 10. The source circuit consists of an n-channel MOSFET BS170, a load resistance of $R_2 = 15\ \Omega$, a capacitance C for stabilization purposes and a constant voltage source that provides the supply voltage v_{CC}. Between the MOSFET's gate and source, a pull down resistor R_1 is placed to ensure the turn-off if no control signal is applied. Experience shows that the BS170's transmission behavior can be approximated by a polynomial of order eight ($K \cong 8$) [10].

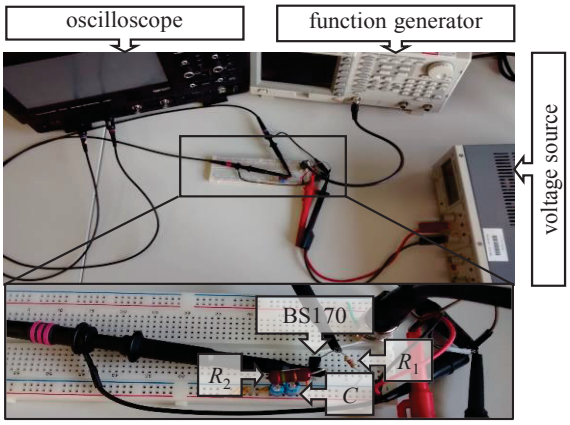

Fig. 9. Measurement test setup with BS170.

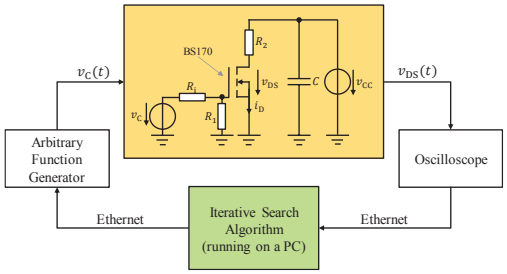

Fig. 10. Illustration of the utilized demonstrator and its measurement environment.

Testing a single parameter combination with the presented measurement setup takes around 15 seconds. This quite long duration is mainly caused by slow remote control of function generator and oscilloscope. It is assumed that this duration can be reduced with faster instruments and communication to some milliseconds.

A. Determination of the demanded output signal

At first, a desired output signal $v_{\mathrm{DS,target}}(t)$ needs to be determined. To do so, the BS170 is initially controlled by a trapezoidal gate-source voltage $v_{\mathrm{GS}}(t)$. The resulting drain-source voltage $v_{\mathrm{DS}}(t)$ is depicted in Fig. 11 (top). Its spectrum $V_{\mathrm{DS}}(f)$ is depicted in Fig. 11 (bottom). Here, all harmonics higher than $5f_0$ shall be removed. Again, due to the Gibbs phenomenon, it is helpful to investigate whether the demanded output signal $v_{\mathrm{DS,target}}(t)$ complies with the source circuit's properties. Here, the demanded output signal $v_{\mathrm{DS,target}}(t)$ is limited by the supply voltage v_{CC} and the maximum drain current $i_{\mathrm{D,max}}$. Therefore, $v_{\mathrm{DS,target}}(t)$ is limited by v_{CC}, R_2 and the BS170's $R_{\mathrm{DS(on)}} \approx 5\ \Omega$ [11]. The demanded output signal $v_{\mathrm{DS,target}}(t)$ is depicted in Fig. 11 (top). The upper limit given by v_{CC} is not exceeded, because the DC offset of $v_{\mathrm{DS,target}}(t)$ is -compared to $v_{\mathrm{DS}}(t)$- slightly reduced. The resulting undershoots of $v_{\mathrm{DS,target}}(t)$, depicted in Fig. 11 (top), are not critical because the resulting drain current is below its maximum possible value $i_{\mathrm{D,max}}$, given by (10).

$$i_{\mathrm{D,max}} = \frac{v_{\mathrm{cc}}}{R_2 + R_{\mathrm{DS(on)}}} \tag{10}$$

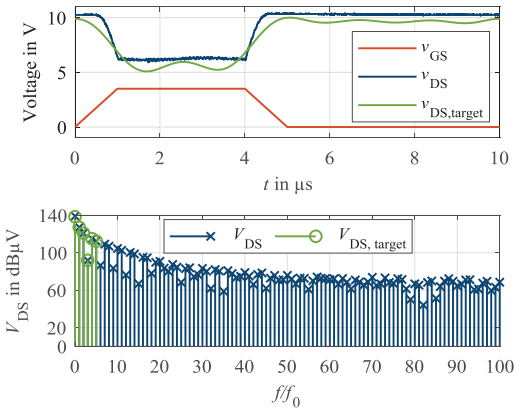

Fig. 11. Measurement: trapezoidal $v_{\mathrm{GS}}(t)$ with resulting $v_{\mathrm{DS}}(t)$ and demanded $v_{\mathrm{DS,target}}(t)$ (top). Comparison of the corresponding output spectra (bottom).

B. Measurement results

$v_{GS}(t)$ is optimized in the frequency range from DC to $5f_0$ ($N = 5$) with $R = 10$ parameter net refinements in $X = 2$ sweeps. The amount of all tested parameter combinations is given by (9) and results in a total number of $Z = 2112$. To test all these parameter combinations, nearly 9 hours were needed. Optimized hardware should be able to reduce this time to some seconds.

As depicted in Fig. 12, the optimized drain-source voltage $v_{DS,optimized}(t)$ is quite similar to the demanded drain-source voltage $v_{DS,target}(t)$. Comparing the spectra $V_{DS}(f)$ and $V_{DS,optimized}(f)$ in Fig. 12 (bottom) and in Fig. 13, the optimized output spectrum $V_{DS,optimized}(f)$ shows significantly reduced frequency components starting from around $7f_0$. The deviation between the original spectrum $V_{DS}(f)$ and the optimized spectrum $V_{DS,optimized}(f)$ between DC and $20f_0$ is depicted in Fig. 13. The frequency components of all three spectra nearly equal each other in range from DC to $5f_0$. Here, no EMC requirements are given. The first frequency component $6f_0$ that is actually intended to be reduced, is reinforced about +13.6 dB instead. This is due to the nonlinear system behavior. The frequency components in this transition region represent intermodulation or harmonic frequencies of the input signal. All higher undesired frequency components with relevant signal level are reduced about - 15 dB to -50 dB. Here, EMC requirements are met.

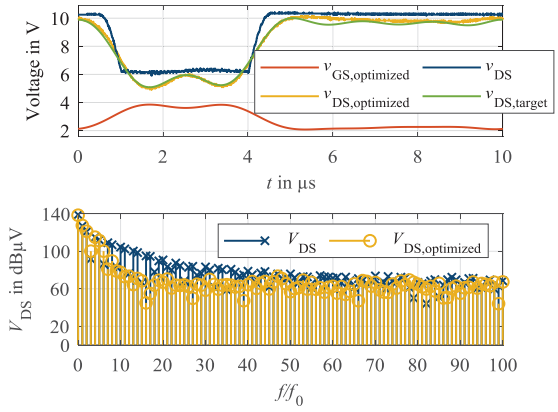

Fig. 12. Measurement: original, demanded and optimized output signal in time domain (top). Spectra $V_{DS}(f)$ and $V_{DS,optimized}(f)$ (bottom).

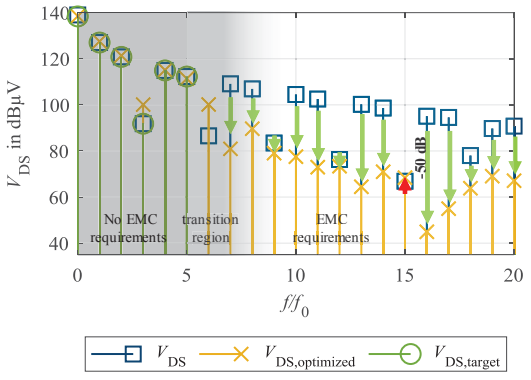

Fig. 13. Measurement: spectra of the original, demanded and optimized output signal.

VI. Conclusion and Outlook

In this work, a new control strategy for nonlinear systems has been introduced. Synthesized control signals have been applied to the gate of a MOSFET in a source circuit to mitigate harmonics of high order. For the determination of the necessary signals, an iterative approach has been developed that enables the optimization of complex nonlinear systems in regard to specific requirements. The proposed optimization algorithm has been demonstrated for a simple source circuit in a simulation and a measurement setup. The optimization algorithm does not require an elaborate identification of the system's behavior. Otherwise bothersome effects, like frequency or temperature dependencies, are intrinsically taken into account by the algorithm. The major downfall is the rather long optimization time that results from the high dimension and wide parameter range of the fundamental problem.

Currently, the algorithm is being developed further to reduce the number of iterations and the run-time of the process. The optimization algorithm can be applied to setups with typical switching frequencies of, e.g., 100 kHz. Therefore, an application to, e.g., a DC/DC converter is reasonable and shall be subject of future investigations.

VII. References

[1] H. C. P Dymond, D. Liu, J. Wang, J. J. O. Dalton and B. H. Stark, "Multi-level active gate driver for SiC MOSFETs," *2017 IEEE Energy Conversion Congress and Exposition (ECCE)*, Cincinnati, Ohio, USA, 1-5 Oct. 2017, pp. 5107-5112.

[2] H. C. P. Dymond, J. Wang, D. Liu, J. J. O. Dalton, N. McNeill, D. Pamunuwa, S. J. Hollis and B. H. Stark, "A 6.7-GHz active gate driver for GaN FETs to combat overshoot, ringing, and EMI," *IEEE Trans. Power Electronics*, vol. 33, no. 1, Jan. 2018.

[3] A. Paredes, V. Sala, H. Ghorbani and L. Romeral, "A novel active gate driver for silicon carbide MOSFET," *IECON 2016 – 42nd Annual Conference of the IEEE Industrial Electronics Society*, Florence, Italy, 23-26 Oct. 2016, pp. 3172-3177.

[4] M. V. Krishna and K. Hatua, "Closed loop analog active gate driver for fast switching and active damping of SiC MOSFET," *2018 IEEE Applied Power Electronics Conference and Exposition (APEC)*, San Antonio, Texas, USA, 4-8 March 2018, pp. 3017-3021.

[5] M. Ebli and M. Pfost, "A novel gate driver approach using inductive feedback to increase the switching speed of power semiconductor devices," *2017 19th European Conference on Power Electronics and Applications (EPE'17 ECCE Europe)*, Warsaw, Poland, 11-14 Sept. 2017, pp. 1-7.

[6] M. Ebli and M. Pfost, "A gate driver approach using inductive feedback to decrease the turn-on losses of power transistors," *PCIM Europe 2018; International Exhibition and Conference for Power Electronics, Intelligent Motion, Renewable Energy and Energy Management*, Nuremberg, Germany, 5-7 June 2018, pp. 396-401.

[7] M. Ebli, M. Wattenberg and M. Pfost, "A gate driver approach enabling switching loss reduction for hard-switching applications," *2017 IEEE 12th International Conference on Power Electronics and Drive Systems (PEDS)*, Honolulu, Hawaii, 12-15 Dec. 2017, pp. 968-971.

[8] A. Bendicks, T. Dörlemann, S. Frei, N. Hees and M. Wiegand, "Active EMI reduction of stationary clocked systems by adapted harmonics cancellation," *IEEE Trans. EMC*, Early Access, pp. 1-9, Aug. 2018.

[9] A. Bendicks and S. Frei, "Broadband noise suppression of stationary clocked DC/DC converters by injecting synthesized and synchronized cancellation signals," *IEEE Trans. Power Electron.*, Early Access, Jan. 2019.

[10] C. Krause, A. Bendicks, T. Dörlemann, S. Frei, „Synthesis of an optimized control signal for an improved EMC switching behavior of MOSFETs using a system characterization approach," in *EMC Europe*, Barcelona, Spain, 2-6 Sept. 2019, unpublished.

[11] On Semiconductor, "BS170 – Small Signal MOSFET 500 mA, 60 Volts," Datasheet.